Check for updates

View Article Online
View Journal

PCCP

Accepted Manuscript

This article can be cited before page numbers have been issued, to do this please use: S. Few, C. Chia, D. Teo, J. Kirkpatrick and J. Nelson, *Phys. Chem. Chem. Phys.*, 2017, DOI: 10.1039/C7CP00317J.



This is an Accepted Manuscript, which has been through the Royal Society of Chemistry peer review process and has been accepted for publication.

Accepted Manuscripts are published online shortly after acceptance, before technical editing, formatting and proof reading. Using this free service, authors can make their results available to the community, in citable form, before we publish the edited article. We will replace this Accepted Manuscript with the edited and formatted Advance Article as soon as it is available.

You can find more information about Accepted Manuscripts in the author guidelines.

Please note that technical editing may introduce minor changes to the text and/or graphics, which may alter content. The journal's standard Terms & Conditions and the ethical guidelines, outlined in our author and reviewer resource centre, still apply. In no event shall the Royal Society of Chemistry be held responsible for any errors or omissions in this Accepted Manuscript or any consequences arising from the use of any information it contains.

ROYAL SOCIETY OF CHEMISTRY

rsc.li/pccp

CREATED USING THE RSC LaTeX PCCP ARTICLE TEMPLATE – SEE www.rsc.org/electronicfiles FOR DETAILS
View Article Online
DOI: 10.1039/C7CP02417J
ARTICLE TYPE www.rsc.org/xxxxxx | XXXXXXXX

The impact of chemical structure and molecular packing on the electronic polarisation of fullerene arrays†

Sheridan Few,*[a] Cleaven Chia,[a,b] Daniel Teo,[a] James Kirkpatrick[a], and Jenny Nelson*[a]

Received Xth XXXXXXXXXX 20XX, Accepted Xth XXXXXXXXX 20XX

First published on the web Xth XXXXXXXXXX 200X

DOI: 10.1039/b000000x

Electronic polarisation contributes to the electronic landscape as seen by separating charges in organic materials. The nature of electronic polarisation depends on the polarisability, density, and arrangement of polarisable molecules. In this paper, we introduce a microscopic, coarse-grained model in which we treat each molecule as a polarisable site, and use an array of such polarisable dipoles to calculate the electric field and associated energy of any arrangement of charges in the medium. The model incorporates chemical structure via the molecular polarisability and molecular packing patterns via the structure of the array. We use this model to calculate energies of charge pairs undergoing separation in finite fullerene lattices of different chemical and crystal structures. The effective dielectric constants that we estimate from this approach are in good quantitative agreement with those measured experimentally in C_{60} and phenyl-C_{61}-butyric acid methyl ester (PCBM) films, but we find significant differences in dielectric constant depending on packing and on direction of separation, which we rationalise in terms of density of polarisable fullerene cages in regions of high field. In general, we find lattices containing molecules of more isotropic polarisability tensors exhibit higher dielectric constants. By exploring several model systems we conclude that differences in molecular polarisability (and therefore, chemical structure) appear to be less important than differences in molecular packing and separation direction in determining the energetic landscape for charge separation. We note that the results are relevant for finite lattices, but not necessarily for infinite systems. We propose that the model could be used to design molecular systems for effective electronic screening.

1 Introduction

[a] *Centre for Plastic Electronics, Department of Physics, Imperial College London, London SW7 2AZ, UK. E-mail: sheridan.few@imperial.ac.uk, jenny.nelson@imperial.ac.uk*
[b] *Now at John A. Paulson School of Engineering and Applied Sciences, Harvard University, 29 Oxford Street, Cambridge, Massachusetts 02138, USA.*

Published on 23 June 2017. Downloaded by Imperial College London Library on 26/06/2017 12:21:41.
Physical Chemistry Chemical Physics Accepted Manuscript

View Article Online
DOI: 10.1039/C7CP00317J

Published on 23 June 2017. Downloaded by Imperial College London Library on 26/06/2017 12:21:41.

Physical Chemistry Chemical Physics Accepted Manuscript

The efficiency of generation of free charges from a photoexcited excitonic state is an important factor in determining the power conversion efficiency of an organic photovoltaic (OPV) or photodetector device. A simple Coulombic picture, treating electrons and holes as point charges, and assuming a relative dielectric constant (ϵ_r) of 3 - 4 and an initial separation (r_{eh}) of 1 - 2 nm between charges, results in an energetic cost $E_{Binding}$ of $\sim$ 0.2 - 0.5 eV associated with the separation of charges. In atomic units

$$E_{Binding} = \frac{e^2}{\epsilon_r r_{eh}} \tag{1}$$

(We use atomic units for consistency with later expressions; in SI units Equation 1 reads $E_{Binding} = \frac{e^2}{4\pi\epsilon_0\epsilon_r r_{eh}}$, as usual.) The value of $E_{Binding}$ is significantly larger than the average thermally available energy at room temperature, $E_{Thermal} \sim$ 0.025 eV. However, many experimental studies have found charge separation efficiencies approaching 100%.[1,2] This surprising observation has stimulated a large body of experimental and theoretical research on the mechanisms and dynamics of charge generation, and the nature of states involved, reviewed in detail in references[3–7]. Alongside other factors, the polarisable medium surrounding charges, and its influence on the energetic landscape for separation of charges, is widely acknowledged to play an important role in determining the efficiency of charge generation. As such, a detailed understanding of the nature of this medium at the molecular scale could play a crucial role in the design of materials for more efficient OPV devices[3–7].

Polarisation of a dielectric medium in response to an electric field may take place through a number of physical processes associated with different timescales[8,9]. Electronic polarisation, a redistribution of the electron clouds surrounding atomic nuclei, typically takes place on a femtosecond timescale comparable to the time period of a visible photon. Atomic polarisation, changes in bond lengths resulting in a redistribution in the positions of atoms and associated partial charges, typically takes place on a picosecond timescale, comparable to the time period of IR radiation. Dipolar polarisation, associated with the rotation of permanent dipoles in a molecule, and ionic rearrangement, the redistribution of mobile ions in a material, typically take place on still longer nanosecond timescales (if species capable of such polarisation are present in the material). When a charge is placed within a polarisable medium, it will polarise its surroundings, thus stabilising the charge relative to the energy this charge would possess in a vacuum; the charge together with the resulting distortion of its nuclear and electronic environment is referred to as a polaron. The spatial extent of the polaron state (determined partly by electronic transfer integrals with neighbouring molecules), and the speed with which it moves within a medium, will determine which forms of polarisation are activated during the creation and transport of that polaron. As charge generation has been reported on timescales of $\sim$100 fs in a wide range of organic photovoltaic blends[3,10–25] , we choose in this study to focus on the role of electronic polarisation, which will be activated on such rapid timescales.

In the limit of a homogeneous continuous medium, screening of the Coulomb interaction via polarisation is included in equation 1 through the ϵ_r term. However, a spatially uniform ϵ_r is only appropriate for materials whose electronic response can

View Article Online
DOI: 10.1039/C7CP00317J

Published on 23 June 2017. Downloaded by Imperial College London Library on 26/06/2017 12:21:41.

reasonably be considered linear, isotropic, and homogeneous. Whilst this may be a fair approximation for large scale systems such as capacitors where bulk effects are important, it may not accurately describe the polarisation of the medium surrounding a bound charge pair in a molecular solid. The positions and orientations of molecules, along with their charge distributions and polarisabilities, can have a large impact on the energetic landscape for charge separation[26,27], and a bulk dielectric model has been shown to be insufficient to accurately describe the electrostatic landscape in some organic systems[28].

A number of studies have addressed the effects of electronic polarisation and the energetic landscape for charge separation using more detailed *microscopic* models. Building on pioneering work by Mott and Littleton[29] developing a lattice model for polar crystals and upon a model subsequently developed by Bounds and Munn[30], Bounds and Siebrand[31] calculate dielectric properties associated with the separation of charges in an infinite lattice of crystalline anthracene, treating each molecule as a single polarisable point. Bounds and Siebrand[31] calculate activation energies of charge carrier generation broadly in line with experimental results, and differences in dielectric constant of around 20% depending on direction of separation. D'Avino et al.[32] use a similar model to calculate the dielectric response to a homogeneous electric field of infinite crystals and semi-infinite (in two dimensions) films of C_{60} and a series of acenes, and how this property evolves with film thickness (from one to several monolayers) and to bulk. The study finds significant differences in dielectric response of molecules close to the surface of two-dimensional films and close to the centre of semi-infinite films, which diminishes with a higher number of monolayers in the film. Dielectric response of molecules close to the middle of films larger than $\approx$ three molecular monolayers are close to those in infinite crystals. In acenes, components of the dielectric tensor associated with response to electric fields aligned with the long axis of the molecules are significantly higher than those in other directions, particularly for larger molecules. Verlaak et al.[27] and Linares et al.[33] show that the alignment of molecules at a Pentacene:C_{60} interface plays an important role in defining energetics for charge separation using an electrostatic model, Poelking et al.[34,35] develop a method allowing the calculation of properties of an infinite or semi-infinite crystal, showing that long range electrostatic interactions can be crucial in defining the energetics of charges close to an interface. Yost et al.[36] describe the use of quantum mechanics / molecular mechanics (QM/MM) simulations on molecules close to an interface in representative snapshots of molecular configurations from molecular dynamics simulations, providing an insight into the role which configurational disorder can play in determining interactions between charged species and their environment. Yost et al.[26] subsequently describe a number of ways in which electrostatic effects can alter the energetic landscape at an interface between organic materials, including through changes in dielectric environment, interfacial vacancies, static interfacial fields, and interfacial disorder, and calculate an example of each using a QM/MM method. The development of microscopic models of electrostatic phenomena in organic semiconductors is reviewed by D'Avino et al.[37].

Whilst chemical structure and arrangement of molecules are both known to be important for defining the energetics of charges, there has not yet been a detailed study on the independent impact of each of these factors on the polarisation of the surrounding molecular assembly and the resulting energetic landscape. In this paper, we examine independently the effect of

Physical Chemistry Chemical Physics Accepted Manuscript

View Article Online
DOI: 10.1039/C7CP00317J

Published on 23 June 2017. Downloaded by Imperial College London Library on 26/06/2017 12:21:41.

chemical structure and molecular packing on the energetics in finite molecular crystals. We select fullerenes for this study, owing to their widespread use in organic photovoltaic devices, their crystalisability (and availability of solved crystal structures), their symmetry and the near isotropic nature of their molecular polarisability[38–40], and the range of functionalised forms available, giving rise to different molecular polarisabilities and packing motifs. The high polarisability of fullerene molecules has also been ascribed an important role in generating free charges[41], as has the rapid delocalisation of the electron within fullerene crystallites or highly ordered fullerene domains[42–44].

Whilst the use of a dielectric constant may be too approximate to yield accurate results, an atomistic model of polarisation effects can be too computationally intensive to study effects in large assemblies of molecules used to model experimental systems. To find a compromise for microscopic systems in this study, we develop a coarse-grained model to calculate dielectric properties in large arrays of molecules. Figure 1 illustrates the scheme for a crystal of PCBM. We use this model to elucidate the role of chemical functionalisation, molecular polarisability, packing, and direction of charge separation in defining energetic barrier to charge separation in fullerenes. We consider each charge to be localised on an individual fullerene at any instant. This approximation is widely used in classical treatments of electrostatics in molecular systems such as microelectrostatic models[37] and should be valid when electronic coupling is weak relative to electrostatic interaction energies. In the results described below, we calculate mean dielectric constants that are in good quantitative agreement with experimental values, but find significant differences in dielectric constant depending on packing and on direction of separation, which we rationalise in terms of density of polarisable fullerene cages in regions of high field. In general, we find lattices containing molecules of more isotropic polarisabiliy tensors exhibit higher dielectric constants. An interesting challenge is the design of molecules with higher dielectric constant that could facilitate charge separation. Whilst some prior studies have addressed the control of slow timescale dipolar response theoretically[45] and by practical demonstration[46], those studies focussed on dipolar rather than electronic polarisability. Therefore, we extend our study to explore the effect of chemical structure on electronic polarisability and dielectric constant in a number of hypothetical functionalised fullerene structures, and find that, whilst those molecules with higher molecular polarisability tend to exhibit higher dielectric constants, differences in molecular polarisability, at least for for this family of molecules. appear to be less important than packing and direction of separation.

2 Method

2.1 Calculating Electronic Polarisability

Molecular starting structures are either extracted from crystallographic information files or built using Gaussview Version 5[47]. Geometries are energy minimised, first using Austin Model 1 (AM1)[48], and subsequently using B3LYP/6-31G*,[49,50] with the

Physical Chemistry Chemical Physics Accepted Manuscript

View Article Online
DOI: 10.1039/C7CP00317J

Published on 23 June 2017. Downloaded by Imperial College London Library on 26/06/2017 12:21:41.

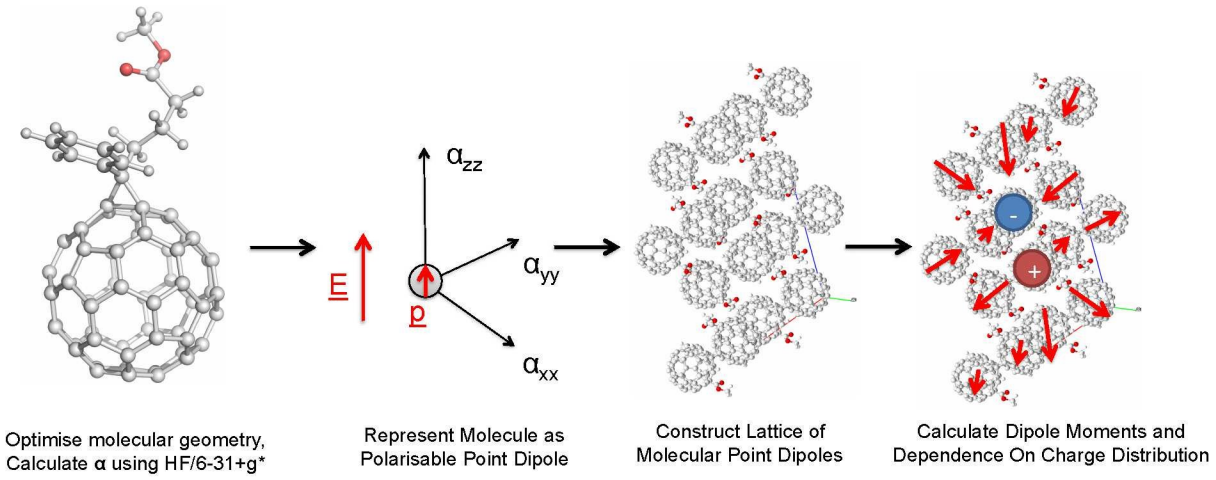


Fig. 1 Schematic of Polarisable Dipole Model

default Berny geometry optimisation algorithm in Gaussian 09.[51] * Electronic polarisabilities are calculated using the Hartree-Fock (HF) method † with the 6-31+G* basis set‡, with the exception of the C_{60} molecule, for which we use the polarisability calculated by Kowalski et al. using a coupled cluster method with the ZPolC basis set.[40] This results in a polarisability 6% higher than that calculated using HF/6-31+G*.

2.2 Molecular Dipole Lattice Model

The basic framework of our model is similar to those of Thole,[60], Applequist[61] and Stern[62]. However, in our case, single polarisable points represent single fullerene molecules rather than single atoms (making the study of large arrays of molecules computationally tractable), and owing to the larger separation of points, no correction is needed to screen the effects of the closest neighbouring dipoles. We consider this coarse-graining justified by the relative symmetry and near-isotropic dielectric tensor of the fullerene molecule, and the relatively large separation of polarisable dipoles.

A lattice is constructed in which each molecule is represented as a single classical polarisable point dipole whose polarisability is calculated as described above. The position and orientation of the polarisability tensor of each dipole in the unit cell are defined according to the crystal structure of the fullerene under consideration, with each point dipole in the centre of mass position of a fullerene cage in the unit cell. (More details of this procedure are provided in supporting information.) A finite lattice is constructed by replicating this unit cell up to a set number of translation vectors. On each molecule, a charge may be placed, which may polarise all surrounding dipoles (except the dipole on the molecule on which the charge sits), which in turn polarise

* Previous studies report that this method gives gives groundstate values for bond lengths and bond angles of a range of organic molecules in good agreement with those measured experimentally.[52–54].

† Previous studies show that the Hartree-Fock method to give results comparable to those calculated with more advanced Møller-Plesset (MP) and coupled cluster methods.[38,40,54–58], and to the Vignale-Kohn functional, a time-dependent current-density-functional theory, expected to give accurate results for polarisability.[59]

‡ This basis set was chosen following a trial study on tetrathiophene, which found a change of less that 2% in any polarisability component when using the larger 6-311++G** basis set (See supporting information)

Physical Chemistry Chemical Physics Accepted Manuscript

View Article Online
DOI: 10.1039/C7CP00317J

Published on 23 June 2017. Downloaded by Imperial College London Library on 26/06/2017 12:21:41.

Physical Chemistry Chemical Physics Accepted Manuscript

their neighbours.

Given such a lattice of polarisable points, a single polarisable point i, at a position $\vec{r}_i$ with an electronic polarisability $\boldsymbol{\alpha}_i$, under the influence of an external electric field $\vec{E}_{ext,i}$ will have a dipole moment, $\vec{\mu}_i$ given by:

$$\vec{\mu}_i = \boldsymbol{\alpha}_i \cdot \vec{E}_{ext,i} \tag{2}$$

Under the influence of a second dipole $\vec{\mu_j}$, at a position $\vec{r}_j$, the dipole at point i will be subject to an additional electric field $\vec{E}_{i,j}$:

$$\vec{E}_{i,j} = -\boldsymbol{T}_{ij} \cdot \vec{\mu}_j \tag{3}$$

Where $\boldsymbol{T}_{ij}$ represents the field tensor for dipoles i and j, given, in the absence of an artificial damping factor, by:

$$\boldsymbol{T}_{ij} = \frac{1}{r_{ij}^3}\left(\mathbb{1} - \frac{3}{r_{ij}^2}\vec{r}_{ij} \otimes \vec{r}_{ij}^{T}\right) \tag{4}$$

Where $\mathbb{1}$ is the identity matrix, $\vec{r}_{ij} = \vec{r}_j - \vec{r}_i$, with components x, y, and z in each Cartesian axis, r_{ij} represents the magnitude of $\vec{r}_{ij}$, and $\vec{r}_{ij} \otimes \vec{r}_{ij}^{T}$ is the dyadic product of $\vec{r}_{ij}$ with its transpose:

$$\vec{r}_{ij} \otimes \vec{r}_{ij}^{T} = \begin{bmatrix} xx & xy & xz \\ yx & yy & yz \\ zx & zy & zz \end{bmatrix} \tag{5}$$

For a system of N polarisable points, the dipole moment at point i is given by:

$$\vec{\mu}_i = \boldsymbol{\alpha}_i \cdot \left(\vec{E}_{ext,i} - \sum_{j=1, j\neq i}^{N} \boldsymbol{T}_{ij} \cdot \vec{\mu}_j\right) \tag{6}$$

Applying similar arguments to each other polarisable point in the lattice, and rearranging:

$$\boldsymbol{J} \cdot \boldsymbol{\mu} = \boldsymbol{E}_{ext} \tag{7}$$

Where $\boldsymbol{J}$ is the relay matrix defining interactions between all pairs of polarisable dipoles in the system:

View Article Online
DOI: 10.1039/C7CP00317J

Published on 23 June 2017. Downloaded by Imperial College London Library on 26/06/2017 12:21:41.

$$\boldsymbol{J} = \begin{bmatrix} \boldsymbol{\alpha}_1^{-1} & \boldsymbol{T}_{12} & \cdots & \boldsymbol{T}_{1N} \\ \boldsymbol{T}_{21} & \boldsymbol{\alpha}_2^{-1} & \cdots & \boldsymbol{T}_{2N} \\ \vdots & \vdots & \ddots & \vdots \\ \boldsymbol{T}_{N1} & \boldsymbol{T}_{N2} & \cdots & \boldsymbol{\alpha}_N^{-1} \end{bmatrix} \tag{8}$$

$\boldsymbol{\mu}$ is a column vector containing the dipole moment of all polarisable points in the system:

$$\boldsymbol{\mu} = (\vec{\mu}_1, \vec{\mu}_2, \ldots \vec{\mu}_N)^T \tag{9}$$

and $\boldsymbol{E}_{ext}$ is a column vector containing the applied electric field, resulting from any external field and permanent charges in the system at each point, i (excluding the charge at i, and charges on the same molecule):

$$\boldsymbol{E}_{ext} = (\vec{E}_{ext,1}, \vec{E}_{ext,2}, \ldots \vec{E}_{ext,N})^T \tag{10}$$

We may thus solve for the dipole moment of all polarisable points in the system using Equation 7 by inversion of the $\boldsymbol{J}$ matrix. The total energy of the lattice may then be calculated as:

$$U_{tot} = U_{dd} + U_{qd} + U_{qq} \tag{11}$$

where U_{dd}, U_{qd}, and U_{qq} represent the dipole-dipole, charge-dipole, and charge-charge interaction energies, given by:

$$U_{dd} = {}^1\!/_2 \boldsymbol{\mu} \cdot \boldsymbol{J} \cdot \boldsymbol{\mu} \tag{12}$$

$$U_{qd} = -\boldsymbol{E}_{ext} \cdot \boldsymbol{\mu} \tag{13}$$

$$U_{qq} = -\sum_i^N q_i V_{ext,i} \tag{14}$$

where q_i represents the charge at point i, and $V_{ext,i}$ represents the electric potential associated with the field $\vec{E}_{ext}$, at point i.

Charge-quadrupole interactions are not included in this model. In each case presented here, we compare energetics for systems containing charges in similar positions in the unit cell, for which charge-quadrupole interactions will be identical in an infinite crystal. However, it should be noted that charge-quadrupole interactions can be very important in defining energetic landscapes across an interface between two different materials, or at a grain boundary[34,35].

Physical Chemistry Chemical Physics Accepted Manuscript

View Article Online
DOI: 10.1039/C7CP00317J

Published on 23 June 2017. Downloaded by Imperial College London Library on 26/06/2017 12:21:41.

Physical Chemistry Chemical Physics Accepted Manuscript

2.3 Scalar Representations of Tensors and Normalised Anisotropy

In discussing anisotropic tensors associated with polarisability and dielectric response, it is useful to define a scalar representation of the tensor, and to quantify anisotropy. For a polarisability tensor $\boldsymbol{\alpha}$, a scalar mean value, α_{mean}, may be defined as:

$$\alpha_{mean} = {}^{1}/_{3} tr(\boldsymbol{\alpha}) \tag{15}$$

where $tr(\boldsymbol{\alpha})$ represents the trace of $\boldsymbol{\alpha}$. An alternative method of representing the $\boldsymbol{\alpha}$ tensor as a scalar is as the product of the diagonal components of this tensor, $\alpha_{vol} = \alpha_{xx}\alpha_{yy}\alpha_{zz}$. In most cases we use the former metric, α_{mean}, however in some cases we also include α_{vol} for ease of comparison with other studies. In order to compare polarisability of different structures, we define a metric for mean polarisability normalised to molecule size, α_{mpa}, as:

$$\alpha_{mpa} = \frac{\alpha_{mean}}{N_{la}} \tag{16}$$

where N_{la} is the number of "large" (ie. non-hydrogen) atoms in the molecule. Normalised anisotropy, A^2, of the tensor $\boldsymbol{\alpha}$ is defined as:

$$A^2 = \frac{(\alpha_{xx} - \alpha_{yy})^2 + (\alpha_{yy} - \alpha_{zz})^2 + (\alpha_{zz} - \alpha_{xx})^2}{2\alpha_{mean}^2} \tag{17}$$

Normalisation is chosen such that $A^2 = 1$ for a tensor with only one nonzero diagonal component, while $A^2 = 0$ for a completely isotropic tensor ($\alpha_{xx} = \alpha_{yy} = \alpha_{zz}$) .

The molecular dipole lattice model is implemented using an in-house Python code, available from the authors upon request. All quantum calculations were performed using the Imperial College High Performance Computing centre clusters.

3 Dielectric Properties of C_{60} Lattices

3.1 Dielectric Properties of C_{60} in a Face Centred Cubic Crystals

We use the coarse-grained model introduced in this paper to estimate ϵ_r as a function of chemical structure and packing in a series of fullerenes. The coarse grained nature of this model allows us to explore this parameter in a range of chemical structures without results being dominated by edge effects, whilst maintaining computational tractability.

First, we study contributions to the electrostatic energy associated with the electronic polarisation response to charge separation in C_{60}. We use the experimentally reported face centred cubic (FCC) crystal structure, with cubic FCC lattices of side lengths $N = 6$, 8, and 10 lattice vectors. In each lattice size, we place a positive charge on a C_{60} molecule close to the centre

View Article Online
DOI: 10.1039/C7CP00317J

Published on 23 June 2017. Downloaded by Imperial College London Library on 26/06/2017 12:21:41.

of a cubic lattice, and a negative charge on a similar molecule in the neighbouring unit cell in the 001 direction. In successive steps, we translate the positive or negative charge by a lattice vector along our chosen direction, and recalculate dipole moments of each molecule, and the energetics of the system.

Figure 2(a) shows the total electrostatic energy, U_{pair} (= U_{tot} in Equation 11 evaluated for a charge pair) in a lattice containing two charges as a function of separation of the charges. U_{pair} may be decomposed into a contribution from the summed polaron binding energy of the two charges, $U_p = U_+ + U_-$, where U_+ and U_- represent the polaron binding energy due to the positive charge alone at its position in the lattice and that due to the negative charge alone at its position in the lattice, respectively, [§] and a contribution from the screened Coulomb binding energy, $U_B = U_{pair} - U_p$ between the two charges. U_p and U_B are isolated as a function of separation of charges in Figures 2(c) and 2(d) respectively.

U_p has only a weak dependence on separation of charges at large $^1/_r$, where charges are close to the centre of the subcrystal, but changes significantly with separation at small $^1/_r$, due to edge effects when charges approach the extremities of the lattice [¶] . The binding energy between the charges (Figure 2(c)) varies in a remarkably linear fashion with $^1/_r$ close to the centre of the lattice, with a slight deviation from linearity at small $^1/_r$. An effective dielectric constant, ϵ_{001}, may be obtained by applying a linear fit to the points in Figure 2(c), and taking the gradient (c.f. Equation 1):

$$\epsilon_x = -\frac{d^1/_{\vec{r}_x}}{dU_B} \tag{18}$$

Where $\vec{r}_x$ represents the displacement in the x direction (001 in this case). We obtain a value of ϵ_{001} in the range 4.3 - 4.7, depending on subcrystal size, and the separation at which we take the gradient (indicated by error bars in Figure 2(d)). This range is comparable to values of 4.08[63], 4.0[64], 4.5[65], 3.85[66] and 3.61[67] extrapolated from optical studies, and 4.4 $\pm$ 0.2 from DC-capacitance measurements [‖ 68]. It is interesting that the value of ϵ_r extracted by this method is consistent over a range of pair separations down to nearest neighbour separations: in other words, the bulk description of binding energy appears valid even over separations where local electric field varies very strongly.

In all subsequent crystals, we calculate ϵ_x using only the three shortest separations, where properties of a charge pair in the bulk are likely to be best approximated.

§ We calculate U_+ and U_- by summing U_{tot}, the total electrostatic energy, of the lattice containing each of the charges individually. We note that, in practice, quadrupole moments are likely to make a significant contribution to absolute values of polaron binding energies, and we calculate U_p here only to isolate U_B from other energetic contributions.

¶ We note that U_B approaches a negative finite value rather than 0 as charges tend towards infinite separation (not observed by Bounds and Siebrand in an infinite lattice[31]). We attribute this phenomenon to edge effects in our finite lattice. We note that U_B approaches closer to 0 for larger lattices under consideration, and that gradient of energy with separation (which is our chief interest here) is relatively insensitive to lattice size.

‖ Lower values in optical studies are to be expected, owing to the short time period associated with optical excitation, which will not be sufficient to allow any form of polarisation but the rearrangement of electrons

Physical Chemistry Chemical Physics Accepted Manuscript

View Article Online
DOI: 10.1039/C7CP00317J

Published on 23 June 2017. Downloaded by Imperial College London Library on 26/06/2017 12:21:41.

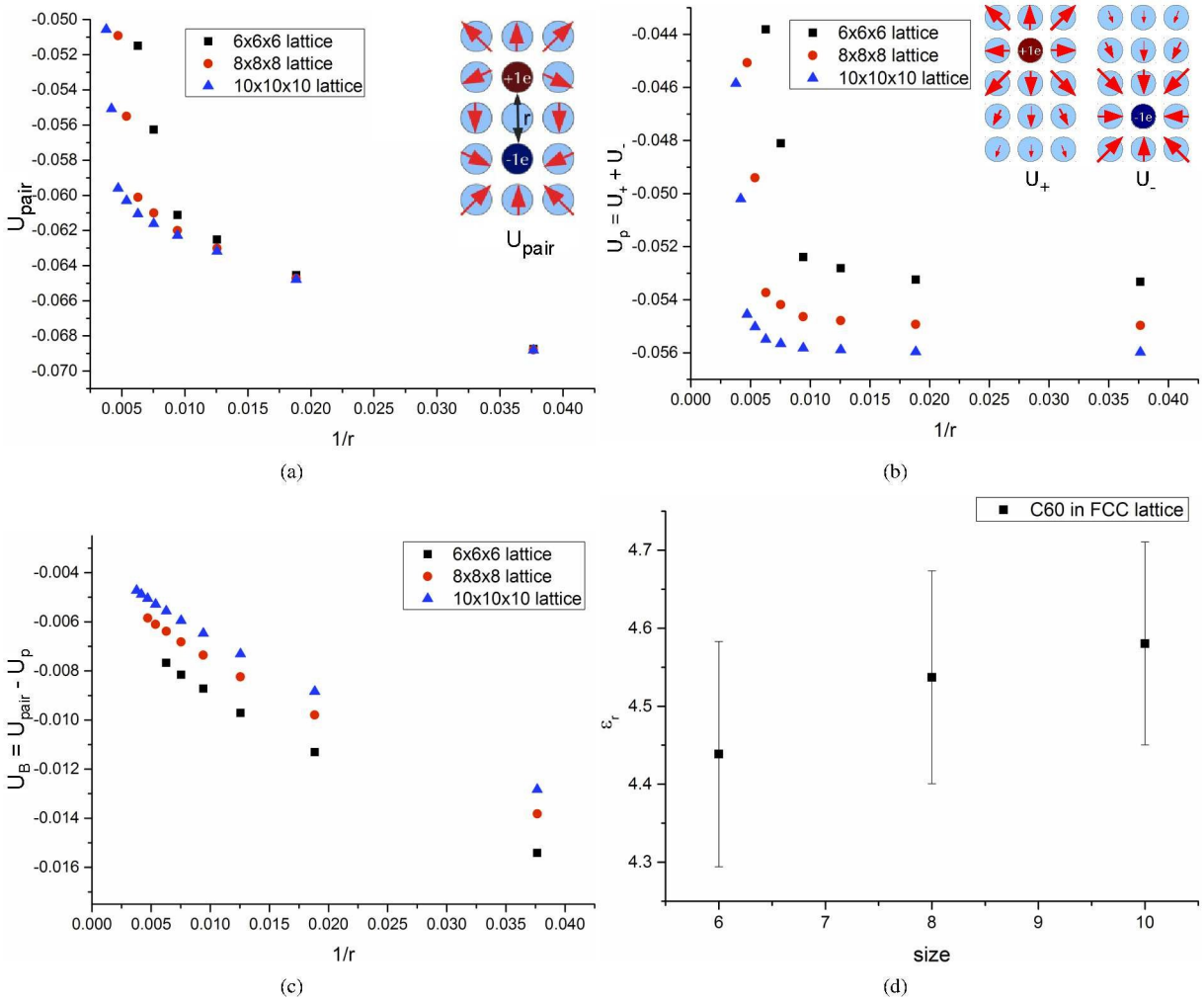


Fig. 2 Separation of Charges in C_{60} in an FCC Lattice Structure (a) Total electrostatic energy in a lattice containing two charges, U_{pair} (b) Sum of polaron binding energy of each charge separately in a lattice, $U_p = U_+ + U_-$, (c) Coulomb Binding energy, $U_B = U_{pair} - U_p$ for a pair of charges in a lattice, against inverse separation, $^1/_r$, of a positive and negative charge and (d) Dielectric constant obtained from the data in (c) using Equation 18, for C_{60} in FCC lattice structure. Cubic lattices with side lengths of 6, 8, and 10 unit cells are considered. Error bars in (d) indicate deviations from an inverse relationship between binding energy and separation.

Physical Chemistry Chemical Physics Accepted Manuscript

This journal is © The Royal Society of Chemistry [year]

View Article Online
DOI: 10.1039/C7CP00317J

Published on 23 June 2017. Downloaded by Imperial College London Library on 26/06/2017 12:21:41.

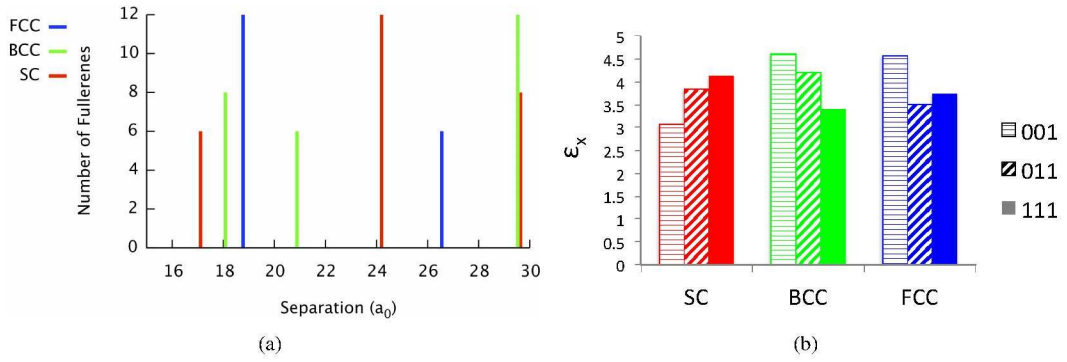


Fig. 3 Dielectric Properties and Radial Distribution of Molecule Centres of C_{60} in Density Scaled FCC, BCC, and SC Lattice Structures Number densities of each structure are scaled to match that of experimentally reported FCC lattice structures, such that cubic side length = 26.56 r_{Bohr}, 20.94 r_{Bohr}, and 16.96 r_{Bohr} in FCC, BCC, and SC lattices respectively (more details in supporting information). (a) Radial distribution of molecule centres in considered FCC, BC, and SC lattice structures. (b) Dielectric constant, ϵ_x, calculated using Equation 18 for three charge separations closest to the centre of the lattice, along 001, 011, and 111 axes, in FCC, BCC and SC lattices. FCC is considered in a cubic lattice with a side length of 10 lattice vectors. BCC and SC lattice sizes were chosen as such that they have a similar number of molecules. As a result BCC, and SC lattices have unequal numbers of lattice vectors in each direction ($8 \times 16 \times 16$ in BCC, $12 \times 18 \times 18$ in SC).

3.2 Dielectric Properties of C_{60} in Body Centred and Simple Cubic Lattices

In order to explore the importance of arrangement of molecules in defining the dielectric properties of a system, we compare effective dielectric constants of C_{60} molecules in the largest FCC lattice ($N = 10$) to those in body centred cubic (BCC) and simple cubic (SC) crystal structures of a similar total number of molecules. In order to study the effect of crystal structure independent of number density, the lattice constant of BCC and SC structures are scaled to yield a fullerene density equal to that of the FCC lattice (details of this scaling procedure are provided in the supporting information). By the Clausius-Mossotti relation,[69] dielectric constant may be expected to scale with molecule density. The point of this study is not to model true polymorphs of C_{60} but to explore the effect of crystal structure alone on effective ϵ_r for a given, isotropic molecular polarisability and a given molecule density. In each lattice, we separate charges along the principal axis (001), and two non-principal axes (011 and 111), in a similar manner to that described in the previous section. Radial distribution of molecule centres in each of these structures is presented in Figure 3(a), and ϵ_x for $x = 001$, 011, and 111 in Figure 3(b).

Figure 3(a) shows that the SC structure has the shortest distance between nearest neighbours in the scaled structure, followed by BCC and then FCC. This might imply a stronger interaction, and a tendency towards a higher dielectric constant. However, in the SC structure, each molecule has only six nearest neighbours, whilst in the BCC and FCC structures, each molecule has eight and twelve respectively. As such, the increase in screening expected in the SC structure due to a stronger nearest-neighbour interaction might be mitigated by the reduced number of nearest neighbours.

We find that differences in crystal structure can cause significant differences in the dielectric properties of the material (see Figure 3(b)). Interestingly, we find ϵ_x to be lowest along the nearest neighbour direction in each case (011 in FCC, 111 in

Physical Chemistry Chemical Physics Accepted Manuscript

View Article Online
DOI: 10.1039/C7CP00317J

Published on 23 June 2017. Downloaded by Imperial College London Library on 26/06/2017 12:21:41.

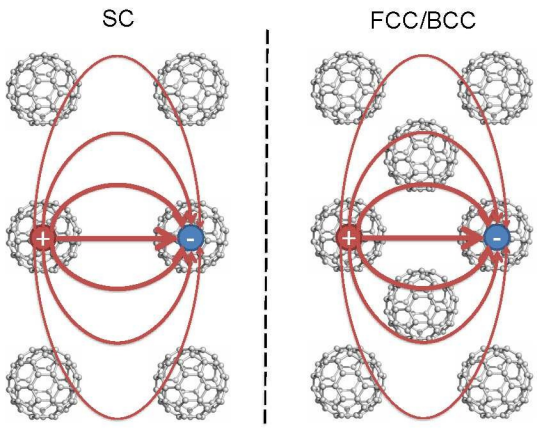


Fig. 4 Schematic of High Field Regions in a C_{60} Slice Containing a Pair of Charges in SC (left) and FCC or BCC (right) Lattices The left panel shows the SC structure sliced along 100 while the right panel shows FCC sliced along 110 (or alternatively BCC (slightly skewed) sliced along 111). Charges are separated along the 001 direction in each case. The red lines indicate approximate direction of electric field of the charge pair in the absence of surrounding molecules, and their thickness represents relative magnitude of the electric field at these points.

BCC, and 001 in SC). We rationalise these differences in terms of a higher proportion of fullerenes in regions of high field when separating along non nearest neighbour directions. We illustrate this principle for separation of charges along the 001 axis in SC compared to FCC or BCC in Figure 4. Similar reasoning applies for 011 in FCC or 111 in BCC lattices. In all cases, we find U_B for a charge pair separated by a single unit cell to be least negative when charges are separated in directions of lowest ϵ_x (values presented in supporting information), consistent with the physical requirement of U_B tending to zero as distance between charges tends to infinity.

We note that the quantity ϵ_x calculated here describes an effective dielectric constant associated with the change in Coulomb energy when separating charges between sites on a lattice. This differs from the dielectric tensor, used to describe the bulk response of a linear, homogeneous medium to an applied electric field. This quantity is suited to describing polarisation when the electric field varies on a length scale much larger than the lattice constant, and will be isotropic for the infinite simple cubic lattice, as described by the Clausius-Mossotti relation[69,70]. We attribute the difference between these quantities to local anisotropy in electric field resulting from differences in arrangement of charges when separating along different lattice vectors.

We find the effective dielectric tensor associated with separation of charges along principal axes in SC, FCC, and BC lattices to be relatively insensitive to lattice size for cubic lattices containing between $\sim$ 1000 and $\sim$ 5000 fullerene molecules (see supporting information), suggesting that our system is close to convergence. However, long range interactions can be important in determining electrostatic properties, as shown by Poelking et al.[34] (albeit chiefly owing to differences in charge-quadrupole interactions between positions in this case, which will be zero in an infinite lattice containing no interface), and it is not possible to rule out any impact of the finite lattice size on our results.

Having calculated dielectric properties of C_{60}, we move on to consider the functionalised fullerene, PCBM, a more relevant

Physical Chemistry Chemical Physics Accepted Manuscript

This journal is © The Royal Society of Chemistry [year]

View Article Online
DOI: 10.1039/C7CP00317J

material for solution processable OPVs, but with a more complex packing motif, and with an anisotropic polarisability tensor.

4 Dielectric Properties of Functionalised Fullerene Lattices

4.1 Dielectric Properties of PCBM in a range of Crystal Structures

We calculate dielectric properties for PCBM in a solvent-free (SF) crystal structure,[71], and in the crystal structures derived for samples crystallised from solutions of chlorobenzene (CB) and ortho-dichlorobenzene (o-DCB)[72]. Unit cells for each structure are shown in Figure 5. In order to address the influence of crystal structure exclusively, we scale lattice constants such that the number density of molecules in CB and o-DCB lattices is the same as in the SF structure (See supporting information for details). In order to exclusively consider the influence of packing and fullerene structure, we do not include solvent molecules in our calculation. Whilst these molecules may have some impact on dielectric properties of the lattice, their electronic polarisability is likely to be much smaller than that of the fullerene molecule owing to their relative size.

We place a positive charge on the PCBM molecule labelled '1' in Figure 5 in a central unit cell, and a negative charge on the corresponding PCBM molecule in a neighbouring unit cell in our chosen direction of separation. In successive steps, we translate the positive or negative charge by a lattice vector along the chosen direction, and recompute U_B. We calculate ϵ_x for each principal axis $x = a, b, c$, as described in Section 3.1, and present results in Figure 5(bottom left).

We find a degree of anisotropy in the dielectric properties in PCBM in CB and o-DCB crystal structures, but a significantly larger anisotropy in the SF lattice. This anisotropy in the dielectric tensor remains, and is even enhanced, when the molecular polarisability tensor is replaced by an *isotropic* tensor of the same α_{mean} (case 'SF(iso)' in figure 5). This implies that the anisotropy of the dielectric tensor stems chiefly from the anisotropic distribution of fullerene cage centres and not from the anisotropy of the polarisability tensor of the molecule. In addition, we find ϵ_r to be higher in all directions when using an isotropic polarisability tensor. This suggests that isotropy of molecular polarisability tensors might be an important factor for facilitating charge separation.

Inspection of slices through the SF structure viewed along the different lattice vectors (Figure 6(a), (b) and (c)) reveals a close packing of molecules along the $\vec{b}$ direction, relatively loose packing along the $\vec{c}$ direction, and an intermediate packing density in the $\vec{a}$ direction. We suggest that this leads to fewer polarisable fullerene cages in regions of high field when charges are separated in the $\vec{b}$ direction than in the $\vec{a}$ and $\vec{c}$ directions (see Figure 6(d)), to which we tentatively attribute the relatively low ϵ_b calculated in this structure. This is analogous to our explanation for differences in ϵ_{001}, ϵ_{011}, and ϵ_{111} in the different lattices of C_{60}.

Packing motifs in CB and oDCB structures appear similar to that of the SF structure, although the distribution of fullerene cages is somewhat more isotropic than in the SF lattice structure. CB and oDCB structures result in significantly more isotropic ϵ_x than the SF structure, suggesting that quite small changes in packing motif may have a large influence on the energetic landscape

Published on 23 June 2017. Downloaded by Imperial College London Library on 26/06/2017 12:21:41.

Physical Chemistry Chemical Physics Accepted Manuscript

View Article Online
DOI: 10.1039/C7CP00317J

Published on 23 June 2017. Downloaded by Imperial College London Library on 26/06/2017 12:21:41.

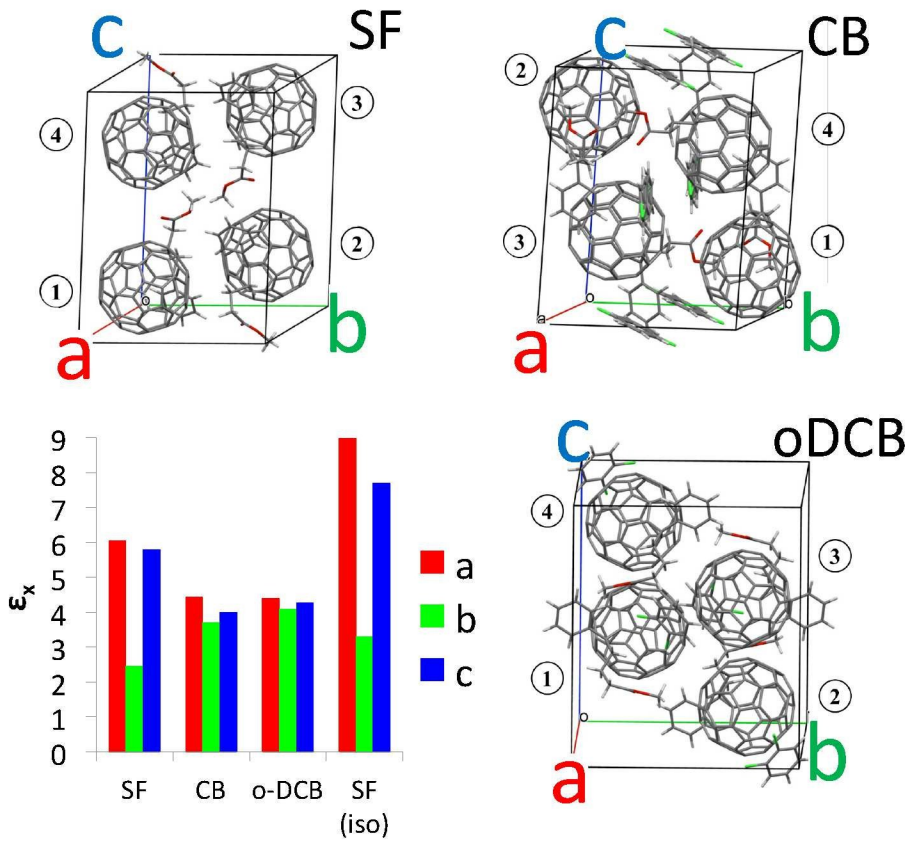


Fig. 5 PCBM crystal structures (Clockwise from top left) Unit cells in a solvent-free (SF) crystal structure as reported by Casalegno et al.[71], and in crystal structures as deposited from CB, and o-DCB as reported by Rispens et al. (lattice parameters provided in supporting information). (Bottom left) Diagonal components of the dielectric tensor along lattice directions a, b, and c, as calculated using Equation 18 for three charge separations closest to the centre of the lattice, for a $12 \times 12 \times 12$ cubic lattice of PCBM in SF, CB and o-DCB lattices, with PCBM molecules represented by anisotropic molecular polarisability tensors, and in SF lattice with PCBM molecules represented by an isotropic molecular polarisability tensor of the same α_{mean}. Number densities of CB and o-DCB lattices scaled to that of SF lattices, such that side lengths are scaled by a factor of 0.986 for the CB lattice, and a factor of 0.961 for the oDCB lattice. Mean values of ϵ_r between the three principal axes are: SF: 4.8, CB: 4.0, oDCB: 4.3, SF(iso) : 6.7. (Lattice parameters in original lattices: SF lattice: $a = 25.5\ r_{Bohr}$, $b = 28.6\ r_{Bohr}$, $c = 36.1\ r_{Bohr}$, $\alpha = 90°$, $\beta = 107.1\ °$, $\gamma = 90\ °$, CB lattice: $a = 26.1\ r_{Bohr}$, $b = 28.9\ r_{Bohr}$, $c = 36.4\ r_{Bohr}$, $\alpha = 80.26°$, $\beta = 78.6\ °$, $\gamma = 80.4\ °$, o-DCB lattice: $a = 26.0\ r_{Bohr}$, $b = 31.4\ r_{Bohr}$, $c = 36.1\ r_{Bohr}$, $\alpha = 90°$, $\beta = 105.3\ °$, $\gamma = 90\ °$.)

Physical Chemistry Chemical Physics Accepted Manuscript

This journal is © The Royal Society of Chemistry [year]

View Article Online
DOI: 10.1039/C7CP00317J

Published on 23 June 2017. Downloaded by Imperial College London Library on 26/06/2017 12:21:41.

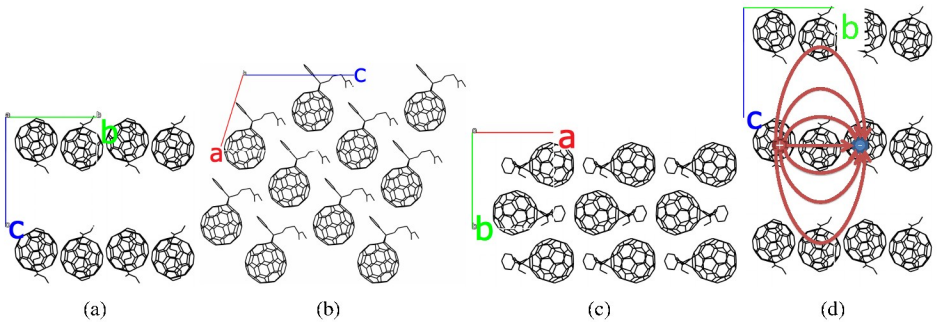


Fig. 6 Slices of PCBM Solvent Free Crystal Structure (a) viewed along $\vec{a}$, sliced between 0.5a and 1.0a, (b) viewed along $\vec{b}$, sliced between 0.0b and 0.5b, (c) viewed along $\vec{c}$, sliced between 0.0c and 0.5c (d) viewed along $\vec{a}$, with lines indicating regions of high field when separating charges in the $\vec{c}$ direction.[71]

for charge separation. We provide similar projections to Figure 6 for CB and oDCB structures in supporting information.

We emphasise that the calculated anisotropy in the effective dielectric tensor chiefly arises from the local field from point charges, and does not describe differences in dielectric response to a homogeneous field. The model we use here is ill-suited to calculating such effects owing to the dominant role edge effects would play when applying a homogenous electric field. The model could, however, be adapted to include periodic boundary conditions in order to consider this effect. As we are predominantly interested in the separation of charges on a molecular scale, we do not model polarisation under a homogeneous field here.

4.2 Designing Functionalised Fullerenes for Low Energetic Barriers to Charge Separation

We have shown that molecular anisotropy and crystal structure can both influence dielectric properties of a molecular system. Next, we explore the extent to which dielectric properties can be enhanced by modifying molecular structure. In order to develop design rules for functionalised fullerenes with high polarisabilities, expected to exhibit low barriers to charge separation, we first calculate the influence of chemical structure on polarisability of a series of molecules. We consider linear conjugated (oligoacetylene and oligoyne) and non-conjugated (alkane and ether) molecules, in addition to cyclic conjugated annulenes, and cyclic non-conjugated crown ethers.

In non-conjugated molecules, we calculate a sublinear increase in electronic polarisability with molecule size at short lengths, which tends to linearity for longer molecules (see Figure 7). We attribute the sublinearity at short lengths to a larger ratio of hydrogen to carbon atoms in shorter molecules, which contribute a small amount to polarisability, but are not included in the normalisation defined in Equation 16. This effect diminishes as the molecule becomes longer. In conjugated linear molecules, we calculate a superlinear increase in polarisability with molecule size. We also calculate a superlinear increase in the annulene series up to ten large atoms. However, ring strain disrupts planarity, π-electron sharing, and polarisability in larger structures.

We note that electronic polarisabilities in ethers are not exceptionally high. Below, we also present calculated electronic

Physical Chemistry Chemical Physics Accepted Manuscript

View Article Online
DOI: 10.1039/C7CP00317J

Published on 23 June 2017. Downloaded by Imperial College London Library on 26/06/2017 12:21:41.

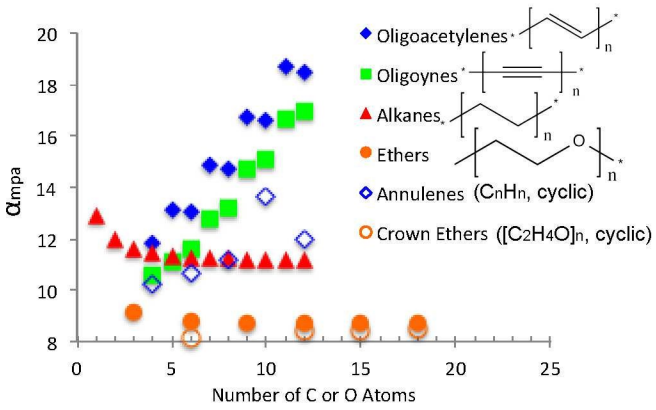


Fig. 7 Polarisabilities of Linear Chain Molecules Mean polarisability per large atom, as defined in Equation 16, for linear conjugated oligacetylenes and oligoynes, linear non-conjugated alkanes and oligoethylene glycols, cyclic conjugated annulenes, and cyclic non-conjugated crown ethers. Chemical structures or formulas also provided. (Compare to α_{mpa} of 8.8 for C_{60} and 9.0 for PCBM, which are likely to be relatively low partly due to lower number of hydrogen atoms in these molecules, which are not included in the normalisation)

Molecule	$\alpha_{mean}(a_0^3)$	α_{vol} (a_0^9)	A^2	α_{mpa}	ϵ_r (expt)
C_{60}	525.1	1.4×10^8	0.000	8.8	3.61, [67]4.08[63] *(optical)*, 4.4± 0.2[68] *(capacitive)*
PCBM	668.4	3.0×10^8	0.004	9.0	3.9 ± 0.1[46] *(optical)*
PTEG-1	735.1	3.9×10^8	0.006	9.1	5.7 ± 0.2 *(capacitive)*
PTEG-2	854.4	6.1×10^8	0.005	9.1	5.3 ± 0.2 *(capacative)*
PCB-Octotetraene	816.8	4.2×10^8	0.019	10.1	NA
PCB-Octane	748.6	5.3×10^8	0.003	9.2	NA

Table 1 Polarisation Properties of Proposed Fullerene Structures Mean polarisability, polarisable volume, anisotropy of polarisability tensor, and mean polarisability per large atom.

polarisability of fullerenes functionalised with ethylene-glycol side groups (PTEG-1 and PTEG-2 fullerenes) for which Torabi et al.[46] report high dielectric permittivities from capacative measurements. These results are consistent with the origin of high dielectric constant in these molecules being the slow rotational response of the molecule rather than the electronic response.

The exceptionally high α_{mpa} we calculate in oligoacetylene chains (α_{mpa} = 14.7 in octotetraene) leads us to propose a new, hypothetical fullerene structure, PCB-Octotetraene (Figure 8, right), resembling PCBM, but with the methyl group replaced with an octotetraene. We also calculate a similar structure, PCBM-Octane (Figure 8, centre), in order to examine the extent to which any enhancement of α_{mpa} in PCB-Octotetraene arises from the π-conjugation of the sidechains (α_{mpa} = 11.2 in octane). The calculated mean polarisabilities and anisotropies of the polarisability tensors for these molecules are given in Table 1. The value of α_{mpa} in PCB-Octotetraene is almost 10% larger than any other fullerene derivative calculated here. We also find higher anisotropy in the polarisability tensor of PCB-Octotetraene than in any other fullerene we consider here. This is likely to be a result of the anisotropy of the polarisability of the octotetraene chain, which is chiefly aligned with its long axis (see supporting information). α_{mpa} in PCB-Octane is not exceptional.

Physical Chemistry Chemical Physics Accepted Manuscript

View Article Online
DOI: 10.1039/C7CP00317J

Published on 23 June 2017. Downloaded by Imperial College London Library on 26/06/2017 12:21:41.

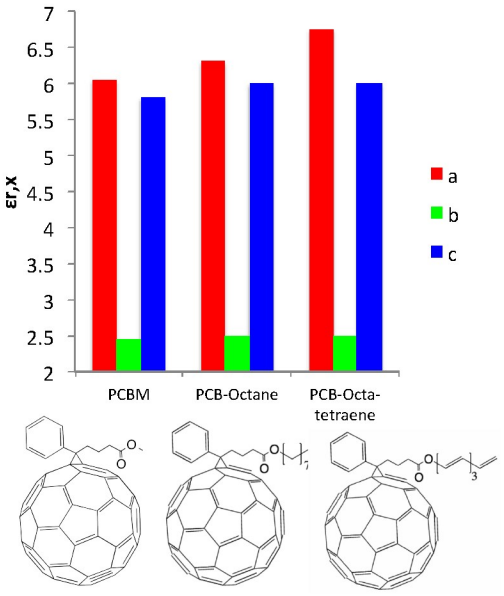


Fig. 8 Chemical Structures of PCBM and Proposed Fullerenes PCB-Octotetraene and PCB-Octane, and Dielectric Properties in a PCBM SF Crystal Structure Diagonal components of the Dielectric tensor along lattice directions a, b, and c, as calculated using Equation 18 for three charge separations closest to the centre of the lattice in a cubic lattice with side lengths of 10 unit cells.

In order to consider how chemical structures tailored to achieve high electronic polarisabilities might behave in a film, we calculate dielectric properties of PCB-Octane and PCB-Octatetraene in a PCBM SF lattice, with PCBM molecules replaced with each of the proposed molecules. In practice, such an arrangement would clearly not be realisable owing to steric hindrance induced by the long (and in the case of PCB-Octotetraene, rigid) sidechains. However, we consider this a useful exercise in considering the extent to which tailoring molecules towards higher electronic polarisabilities could be a promising approach. The components of the resulting dielectric tensor are shown in Figure 8, and isotropic representations of polarisability tensors in Table 1.

The impact of the change in side group on ϵ_r is weak relative to the effect of separation direction. Figure 8 shows an enhanced effective dielectric constant along the a axis in PCB-Octotetraene relative to PCBM and PCB-Octane, but find near-identical effective dielectric constants along the b and c axes among the three molecules. Moreover, the benefit of an isotropic polarisability tensor still appears to outweigh the benefit of a larger but anisotropic polarisability: a comparison of Figure 5 and Figure 8 shows that every component of the calculated dielectric constant of PCBM in a solvent free lattice, but with an isotropic α exceeds every component of the calculated ϵ_r anisotropic PCB-octotetraene, despite the larger mean polarisability for the latter case. Thus, while these results suggest that the design of molecules with higher electronic polarisabilities to provide a more favourable energetic landscape for charge separation is possible, the impact of substitutions on processability, packing motif / packing density and, importantly, on the isotropy of polarisability should also be considered.

Physical Chemistry Chemical Physics Accepted Manuscript

View Article Online
DOI: 10.1039/C7CP00317J

Published on 23 June 2017. Downloaded by Imperial College London Library on 26/06/2017 12:21:41.

Physical Chemistry Chemical Physics Accepted Manuscript

5 Conclusions

In this paper, we present a coarse grained model for the calculation of the electronic polarisation response of a finite fullerene lattice to the presence of charge pair. The model is able to reproduce dielectric constants which are comparable to those reported experimentally in films. However, we note that caution must be taken in using results presented here for finite nanocrystallites to draw conclusions about bulk systems. We show that this model implies large differences in the energetic barrier associated with the rapid separation of charges, depending upon both the packing structure and the direction in which the charges are separated. In fact, our results suggest that molecular packing may be a more crucial factor in determining energetic landscapes than electronic polarisabilities of substituents. We show how the impact of alternative molecular structures (such as new fullerene derivatives) could be modelled and show a high ϵ_r for a hypothetical functionalised fullerene, PCB-Octotetraene.

In realistic systems, in which crystal sizes and orientations are disordered, we might on the basis of these results expect charge separation to favourably occur predominantly at interfaces where molecular orientations are such that ϵ_x are high along the direction of separation. Over longer distances of separation, when disorder is significant, we might expect differences in ϵ_x in different directions to become smaller, and the dielectric tensor to become more isotropic. Other factors, such as the energetic availability of electronically delocalised states over pairs[73–76] or larger numbers of molecules[77–79], change in quadrupolar environment[27,33–35] and energetic disorder at crystal boundaries and heterojunctions[26,80,81], could also likely to play an important role in determining the probability of charge separation, and should not be neglected in a more detailed treatment[3].

By coarse graining the system at the molecular - rather than the atomic - level the method can allow modelling of systems where the charge separation r_{eh} during charge separation is still small compared to the crystallite dimentions. In principle the method can be used to study the effect of structural disorder, chemical impurites and heterogeneous systems (such as donor: acceptor binaries) as well as other molecules and crystal structures. For example, it could be readily compatible with disordered molecular assemblies generated by coarse grained molecular dynamics.[82]

Acknowledgements

JN and SF acknowledge the support of the UK Engineering and Physical Sciences Research Council through the Plastic Electronics Doctoral Training Centre (EP/G037515), the Supergen Supersolar Hub (EP/J017361), and grants EP/P005543 and EP/K030671. CC acknowledges support from the A*STAR National Science Scholarship. JN thanks the Royal Society for a Wolfson Merit Award. We thank Jarvist Frost for useful discussions.

References

1 S. H. Park, A. Roy, S. Beaupre, S. Cho, N. Coates, J. S. Moon, D. Moses, M. Leclerc, K. Lee and A. J. Heeger, *Nature Photonics*, 2009, **3**, 297–303.

View Article Online
DOI: 10.1039/C7CP00317J

Published on 23 June 2017. Downloaded by Imperial College London Library on 26/06/2017 12:21:41.

2 K. Vandewal, S. Albrecht, E. T. Hoke, K. R. Graham, J. Widmer, J. D. Douglas, M. Schubert, W. R. Mateker, J. T. Bloking, G. F. Burkhard, A. Sellinger, J. M. J. Fréchet, A. Amassian, M. K. Riede, M. D. McGehee, D. Neher and A. Salleo, *Nature materials*, 2014, **13**, 63–8.

3 S. Few, J. M. Frost and J. Nelson, *Phys. Chem. Chem. Phys.*, 2015, **17**, 2311–2325.

4 M. A. Loi and A. Troisi, *Physical Chemistry Chemical Physics*, 2014, **16**, 20277–20278.

5 F. Gao and O. Inganäs, *Physical Chemistry Chemical Physics*, 2014, 20291–20304.

6 T. M. Clarke and J. R. Durrant, *Chemical reviews*, 2010, **110**, 6736–6767.

7 D. Beljonne, J. Cornil, L. Muccioli, C. Zannoni, J.-L. Bredas and F. Castet, *Chemistry of Materials*, 2011, **23**, 591–609.

8 E. A. Silinsh and V. Capek, *Organic Molecular Crystals: Interaction, Localization and Transport Phenomena*, American Institute of Physics, 1997.

9 Agilent Technologies, *Basics of Measuring the Dielectric Properties of Materials*, 2014.

10 B. Kraabel, C. Lee, D. McBranch, D. Moses, N. Sariciftci and a.J. Heeger, *Chemical Physics Letters*, 1993, **213**, 389–394.

11 I. Hwang, D. Moses and A. Heeger, *The Journal of Physical Chemistry C*, 2008, **112**, 4350–4354.

12 C.-X. Sheng, T. Basel, B. Pandit and Z. Vardeny, *Organic Electronics*, 2012, **13**, 1031–1037.

13 L. G. Kaake, D. Moses and A. J. Heeger, *The Journal of Physical Chemistry Letters*, 2013, **4**, 2264–2268.

14 S. Mukamel, *The Journal of Physical Chemistry A*, 2013, **117**, 10565.

15 C. Brabec, G. Zerza, G. Cerullo, S. Di Silvestri, S. Luzzati, J. C. Hummelen and S. Sariciftci, *Chemical Physics Letters*, 2001, **340**, 232–236.

16 F. Zhang, K. Jespersen, C. Björström, M. Svensson, M. Andersson, V. Sundström, K. Magnusson, E. Moons, a. Yartsev and O. Inganäs, *Advanced Functional Materials*, 2006, **16**, 667–674.

17 I. W. Hwang, C. Soci, D. Moses, Z. Zhu, D. Waller, R. Gaudiana, C. J. Brabec and A. J. Heeger, *Advanced Materials*, 2007, **19**, 2307–2312.

18 F. Etzold, I. A. Howard, N. Forler, D. M. Cho, M. Meister, H. Mangold, J. Shu, M. R. Hansen, K. Müllen and F. Laquai, *Journal of the American Chemical Society*, 2012, **134**, 10569–83.

19 G. Grancini, M. Maiuri, D. Fazzi, A. Petrozza, H.-J. Egelhaaf, D. Brida, G. Cerullo and G. Lanzani, *Nature Materials*, 2013, **12**, 29–33.

20 N. Banerji, S. Cowan, M. Leclerc, E. Vauthey and A. J. Heeger, *Journal of the American Chemical Society*, 2010, **132**, 17459–17470.

21 N. Banerji, *Journal of Materials Chemistry C*, 2013, **1**, 3052.

22 M. Tong, N. E. Coates, D. Moses, A. J. Heeger, S. Beaupré and M. Leclerc, *Physical Review B*, 2010, **81**, 125210.

23 F. Provencher, N. Bérubé, A. W. Parker, G. M. Greetham, M. Towrie, C. Hellmann, M. Côté, N. Stingelin, C. Silva and S. C. Hayes, *Nature Communications*, 2014, **5**, 4288.

24 E. Villa, H. Li, P. Gregoire, S. M. Tuladhar, M. S. Vezie, S. Few, C. M. Bazan, J. Nelson, C. Silva-Acuna and E. R. Bittner, *Scientific Reports*, 2016, **6**, 29437.

25 S. Gélinas, A. Rao, A. Kumar, S. L. Smith, A. W. Chin, J. Clark, T. S. van der Poll, G. C. Bazan and R. H. Friend, *Science (New York, N.Y.)*, 2014, **343**, 512–6.

26 S. R. Yost and T. Van Voorhis, *The Journal of Physical Chemistry C*, 2013, **117**, 5617–5625.

27 S. Verlaak, D. Beljonne, D. Cheyns, C. Rolin, M. Linares, F. Castet, J. Cornil and P. Heremans, *Advanced Functional Materials*, 2009, **19**, 3809–3814.

28 K. A. Schwarz, R. Sundararaman and T. A. Arias, *The Journal of Chemical Physics*, 2015, **142**, 214101.

29 N. F. Mott and M. J. Littleton, *Transactions of the Faraday Society*, 1938, **34**, 485–499.

30 P. J. Bounds and R. W. Munn, *Chemical Physics*, 1979, **44**, 103–112.

31 P. J. Bounds and W. Siebrand, *Chemical Physics Letters*, 1980, **75**, 414.

32 G. D'Avino, D. Vanzo and Z. G. Soos, *Journal of Chemical Physics*, 2016, **144**, 034702.

33 M. Linares, D. Beljonne, K. Lancaster, J.-l. Bre, S. Verlaak, A. Mityashin, P. Heremans, A. Fuchs, C. Lennartz, P. Aurel and L. Ducasse, *The Journal of*

Physical Chemistry Chemical Physics Accepted Manuscript

View Article Online
DOI: 10.1039/C7CP00317J

Published on 23 June 2017. Downloaded by Imperial College London Library on 26/06/2017 12:21:41.

Physical Chemistry C, 2010, 3215–3224.

34 C. Poelking, M. Tietze, C. Elschner, S. Olthof, D. Hertel, B. Baumeier, F. Würthner, K. Meerholz, K. Leo and D. Andrienko, *Nature Materials*, 2015, **14**, 434–439.

35 C. Poelking and D. Andrienko, *Journal of the American Chemical Society*, 2015, **137**, 6320–6326.

36 S. R. Yost, L.-P. Wang and T. Van Voorhis, *The Journal of Physical Chemistry C*, 2011, **115**, 14431–14436.

37 G. D'Avino, F. Muccioli, L. Castet, C. Poelking, D. Andrienko, Z. G. Soos, J. Cornil and D. Beljonne, *Journal of Physics: Condensed Matter*, 2016, **28**, 433002.

38 D. S. Sabirov, R. R. Garipova and R. G. Bulgakov, *Chemical Physics Letters*, 2012, **523**, 92–97.

39 D. S. Sabirov, A. A. Tukhbatullina and R. G. Bulgakov, *Computational and Theoretical Chemistry*, 2012, 113–117.

40 K. Kowalski, J. R. Hammond, W. a. de Jong and A. J. Sadlej, *The Journal of chemical physics*, 2008, **129**, 226101.

41 D. Veldman, O. Ipek, S. C. J. Meskers, J. Sweelssen, M. M. Koetse, S. C. Veenstra, J. M. Kroon, S. S. van Bavel, J. Loos and R. A. J. Janssen, *Journal of the American Chemical Society*, 2008, **130**, 7721–7735.

42 B. M. Savoie, A. Rao, A. a. Bakulin, S. Gelinas, B. Movaghar, R. H. Friend, T. J. Marks and M. a. Ratner, *Journal of the American Chemical Society*, 2014, **136**, 2876–84.

43 A. A. Y. Guilbert, M. Schmidt, A. Bruno, J. Yao, S. King, S. M. Tuladhar, T. Kirchartz, M. I. Alonso, A. R. Goñi, N. Stingelin, S. a. Haque, M. Campoy-Quiles and J. Nelson, *Advanced Functional Materials*, 2014, **24**, 6972–6980.

44 S. L. Smith and A. W. Chin, *Physical Review B*, 2015, **91**, 201302(R).

45 H. D. de Gier, R. Broer and R. W. A. Havenith, *Physical Chemistry Chemical Physics*, 2014, **16**, 12454–12461.

46 S. Torabi, F. Jahani, I. Van Severen, C. Kanimozhi, S. Patil, R. W. A. Havenith, R. C. Chiechi, L. Lutsen, D. J. M. Vanderzande, T. J. Cleij, J. C. Hummelen and L. J. A. Koster, *Advanced Functional Materials*, 2015, **25**, 150–157.

47 R. Dennington, T. Keith and J. Millam, *Semichem Inc., Shawnee Mission, KS*, 2009.

48 M. J. S. Dewar, E. G. Zoebisch, E. F. Healy and J. J. P. Stewart, *Journal of the American Chemical Society*, 1985, **107**, 3902–3909.

49 A. D. Becke, *The Journal of Chemical Physics*, 1993, **98**, 5648.

50 R. Ditchfield, W. J. Hehre and J. A. Pople, *The Journal of Chemical Physics*, 1971, **54**, 724.

51 M. J. Frisch, G. W. Trucks, H. B. Schlegel, G. E. Scuseria, M. A. Robb, J. R. Cheeseman, G. Scalmani, V. Barone, B. Mennucci, G. A. Petersson, H. Nakatsuji, M. Caricato, X. Li, H. P. Hratchian, A. F. Izmaylov, J. Bloino, G. Zheng, M. Sonnenburg, M. Hada, M. Ehara, K. Toyota, R. Fukuda, J. Hasegawa, M. Ishida, T. Nakajima, Y. Honda, O. Kitao, H. Nakai, T. Vreven, J. Montgomery, J. A., J. E. Peralta, F. Ogliaro, M. Bearpark, J. J. Heyd, E. Brothers, K. N. Kudin, V. N. Staroverov, R. Kobayashi, J. Normand, K. Raghavachari, A. Rendell, J. C. Burant, S. S. Iyengar, J. Tomasi, M. Cossi, N. Rega, M. J. Millam, M. Klene, J. E. Knox, J. B. Cross, V. Bakken, C. Adamo, J. Jaramillo, R. Gomperts, R. E. Stratmann, O. Yazyev, A. J. Austin, R. Cammi, C. Pomelli, J. W. Ochterski, R. L. Martin, K. Morokuma, V. G. Zakrzewski, G. A. Voth, P. Salvador, J. J. Dannenberg, S. Dapprich, A. D. Daniels, Ö. Farkas, J. B. Foresman, J. V. Ortiz, J. Cioslowski and D. J. Fox, *Gaussian, Inc., Wallingford CT*, 2009.

52 K. Houk, P. Lee and M. Nendel, *The Journal of Organic Chemistry*, 2001, 5517–5521.

53 K. E. Riley, B. T. Op't Holt and K. M. Merz, *Journal of Chemical Theory and Computation*, 2007, **3**, 407–433.

54 E. Livshits and R. Baer, *Physical Chemistry Chemical Physics : PCCP*, 2007, **9**, 2932–41.

55 S. J. A. van Gisbergen, P. R. T. Schipper, O. V. Gritsenko, E. J. Baerends, J. G. Snijders, B. Champagne and B. Kirtman, *Physical Review Letters*, 1999, **83**, 694–697.

56 F. A. Bulat, A. Toro-Labbé, B. Champagne, B. Kirtman and W. Yang, *The Journal of chemical physics*, 2005, **123**, 014319.

57 V. Lacivita, M. Rèrat, R. Orlando, M. Ferrero and R. Dovesi, *The Journal of chemical physics*, 2012, **136**, 114101.

Physical Chemistry Chemical Physics Accepted Manuscript

View Article Online
DOI: 10.1039/C7CP00317J

Published on 23 June 2017. Downloaded by Imperial College London Library on 26/06/2017 12:21:41.

58 M. Huzak and M. S. Deleuze, *The Journal of chemical physics*, 2013, **138**, 024319.

59 M. van Faassen, P. de Boeij, R. van Leeuwen, J. Berger and J. Snijders, *Physical Review Letters*, 2002, **88**, 186401.

60 B. Thole, *Chemical Physics*, 1981, **59**, 341–350.

61 J. Applequist, J. R. Carl and K.-k. Fung, *Journal of the American Chemical Society*, 1972, **261**, 2952–2960.

62 H. A. Stern, G. A. Kaminski, J. L. Banks, R. Zhou, B. J. Berne and R. A. Friesner, *The Journal of Physical Chemistry B*, 1999, **103**, 4730–4737.

63 P. C. Eklund, A. M. Rae, Y. Wang, P. Zhou, K.-A. Wang, J. M. Holden, M. S. Dresselhaus and G. Dresselhaus, *Thin Solid Films*, 1995, **257**, 211.

64 A. Richter and J. Sturm, *Applied Physics A*, 1995, **61**, 163–170.

65 P. Milani, M. Manfredini, G. Guizzetti, F. Marabelli and P. M, *Solid State Communications*, 1994, **90**, 639–642.

66 B. Bernardo, D. Cheyns, B. Verreet, R. D. Schaller, B. P. Rand and N. C. Giebink, *Nature Communications*, 2014, **5**, 3245.

67 S. L. Ren, Y. Wang, A. M. Rao, E. McRae, J. M. Holden, T. Hager, K. Wang, W.-T. Lee, H. F. Ni, J. Selegue and P. C. Eklund, *Applied Physics Letters*, 1991, **59**, 2678.

68 A. F. Hebard, R. C. Haddon, R. M. Fleming and A. R. Kortan, *Applied Physics Letters*, 1991, **59**, 2109.

69 J. Hannay, *European Journal of Physics*, 1983, **4**, 141–143.

70 P. B. Allen, *Journal of Chemical Physics*, 2004, **120**, 2951.

71 M. Casalegno, S. Zanardi, F. Frigerio, R. Po, C. Carbonera, G. Marra, T. Nicolini, G. Raos and S. V. Meille, *Chemical Communications (Cambridge, England)*, 2013, **49**, 4525–7.

72 M. T. Rispens, A. Meetsma, R. Rittberger, C. J. Brabec, N. S. Sariciftci and J. C. Hummelen, *Chemical Communications (Cambridge, England)*, 2003, **17**, 2116–8.

73 A. A. Bakulin, A. Rao, V. G. Pavelyev, P. H. M. van Loosdrecht, M. S. Pshenichnikov, D. Niedzialek, J. Cornil, D. Beljonne and R. H. Friend, *Science (New York, N.Y.)*, 2012, **1340**, 1–13.

74 E. B. Isaacs, S. Sharifzadeh, B. Ma and J. B. Neaton, *The Journal of Physical Chemistry Letters*, 2011, **2**, 2531–2537.

75 B. Baumeier, D. Andrienko and M. Rohlfing, *Journal of Chemical Theory and Computation*, 2012, **8**, 2790–2795.

76 S. Few, J. M. Frost, J. Kirkpatrick and J. Nelson, *The Journal of Physical Chemistry C*, 2014, **16**, 8253–8261.

77 D. L. Cheung and A. Troisi, *The Journal of Physical Chemistry C*, 2010, **114**, 20479–20488.

78 B. M. Savoie, A. Rao, A. A. Bakulin, S. Gelinas, B. Movaghar, R. H. Friend, T. J. Marks and M. A. Ratner, *Journal of the American Chemical Society*, 2014, **136**, 2876–84.

79 G. Raos, M. Casalegno and J. Ide, *Journal of Chemical Theory and Computation*, 2013, **10**, 364372.

80 T. Liu, D. L. Cheung and A. Troisi, *Physical Chemistry Chemical Physics : PCCP*, 2011, **13**, 21461–70.

81 Y.-T. Fu, C. Risko and J.-L. Brédas, *Advanced Materials (Deerfield Beach, Fla.)*, 2013, **25**, 878–82.

82 F. Steiner, S. Foster, A. Losquin, J. Labram, T. D. Anthopoulos, J. M. Frost and J. Nelson, *Materials Horizons*, 2015, **2**, 113–119.

Physical Chemistry Chemical Physics Accepted Manuscript